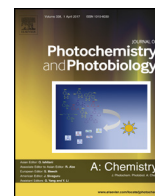




Contents lists available at ScienceDirect

Journal of Photochemistry and Photobiology A: Chemistry

journal homepage: www.elsevier.com/locate/jphotochem

Green synthesis of fluorescent N,O-chelating hydrazone Schiff base for multi-analyte sensing in Cu²⁺, F⁻ and CN⁻ ions

Neeraj Saini^a, Nicha Prigyai^a, Chidchanok Wannasiri^a, Vuthichai Ervithayasuporn^{a,*}, Suda Kiatkamjornwong^{b,c}

^a Department of Chemistry, Center of Excellence for Innovation in Chemistry (PERCH-CIC), Center for Inorganic and Materials Chemistry, Faculty of Science, Mahidol University, Rama VI Road, Ratchathewi District, Bangkok 10400, Thailand

^b Faculty of Science, Chulalongkorn University, Phayathai Road, Bangkok 10330, Thailand

^c FRST, Division of Science, The Royal Society of Thailand, Sanam Suepa, Dusit, Bangkok 10300, Thailand

ARTICLE INFO

Article history:

Received 31 January 2018

Received in revised form 1 March 2018

Accepted 12 March 2018

Available online 13 March 2018

Keywords:

Dehydroacetic acid

1,8-Naphthalimide

Fluorescence

Copper

Fluoride

Cyanide

ABSTRACT

A colorimetric and fluorometric hydrazone Schiff's base derived from dehydroacetic acid by three-steps and high-yield syntheses under green approach employing ethanol as a solvent has been prepared. Multi-analyte sensing for both metal cation (Cu²⁺) and anions (F⁻ and CN⁻), with high sensitivity and competitive selectivity, was encountered. The sensing mechanism of anion detection found to be deprotonation of N–H and O–H moieties in the presence of ions. However, metal cation like copper(II) ions chelation with sensor, leads to diminish intra-molecular charge transfer (ICT) with chelation induced quenching of fluorescence (CHQF). Contrary, anionic interaction ensued in heightened ICT as well as photo-induced electron transfer (PET) processes. The Job's plots interpretation rendered stoichiometry of 2:1 with Cu²⁺/F⁻ and 1:1 with CN⁻. Moreover, the detection limits of 0.962 ppm (Cu²⁺), 0.023 ppm (F⁻) and 0.073 ppm (CN⁻) were much lower than WHO guidelines. Further, either water or methanol was employed to differentiate F⁻/CN⁻ ions with sensor in THF, with prominent visible naked eye and fluorometric responses.

© 2018 Elsevier B.V. All rights reserved.

1. Introduction

Constructing dual responsive chemosensors for the efficient and selective recognition of metal ions as well as anions simultaneously are still a challenging task for the scientific community [1–3]. Nowadays, research scenario has been focused more on developing optical signaling probes due to high competitive selectivity, rapid naked eye detection in ambient light and economical testing, over conventional detection methods [4,5]. Various receptor molecules interacting through unidirectional hydrogen bonding [6,7], ions induced Si–O bond cleavage reactions [8], molecular encapsulation [9], chelation [10] etc. displaying either colorimetric or fluorometric responses, have been contrived and tested toward ions [11]. But the majority of them exhibited severe limitations such as non-discrimination between fluoride and cyanide ions, interference from other competing ions specially acetate ions, long time to response and/or irreversibility [12–15]. On the other side, deprotonation

based sensing probes display higher selectivity with stable optical responses [16,17]. As an example, Pu et al. [18] accounted various diarylethene based chemosensors for fluoride and copper ions in acetonitrile. However, Wan and co-workers described a phenol derived indicator system with dual optical responses toward fluoride and risky cyanide ions. Even though, these systems were excellent examples of chemosensors but effective only in pure organic environments limiting their application to off-site detection. In addition, aqueous analysis suffers from solvent competition and probe insolubility, ensuing sensing of ions an uphill battle [19,20]. Probes that can effectively detect multiple ions in aqueous medium are highly desirable but still quite rare [21,22]. Further, synthetic methodologies followed in the previous reports involve the use of hazardous chemicals such as pyridines, dioxanes, nitrobenzene, etc. with high temperature and tedious extraction processes [1,15,18]. This puts a negative impact on the development of economical sensing probes as well as on human health.

It has been well demonstrated that both metal ions as well as anions are crucial constituents in various biological, manufacturing and metallurgical processes [23–26]. In particular, copper ions act as cofactor and active site constituent in various metalloenzymes due to its versatile redox and binding properties [27–29]. Also, fluoride ions

* Corresponding author.

E-mail address: vuthichai.erv@mahidol.ac.th (V. Ervithayasuporn).

have been a crucial constituent in toothpastes and drinking water. It precludes dental caries [30]. However, over intake of fluoride ions is deduced for many medical ailments such as fluorosis, osteoporosis or even urolithiasis [31,32]. Similarly, excess concentration of cyanide ions poses hazardous impingement on the living systems [33–35]. For these reasons, an impetus always exists for the development of economical optical probes that assist in maintaining a periodic check and in-turn regulate ion's concentration in the ecosystem [36,37].

Majorly, 1,8-naphthalimide moiety has been exploited as fluorophore unit in different sensing systems due to eminent quantum yields, proficient photo-stability and prominent Stokes' shift [38,39]. Moreover, pyran ring systems have evinced biocompatibility, scuttling unexampled dimensions of sensor application in biological system. Additionally, a pyrone derivative such as dehydroacetic acid based receptor system puts forth excellent chelation based sensing of metal ions [40,41]. Literature survey revealed that there is still paucity of dual responsive sensors that can selectively detect copper ions in addition to differentiating fluoride and cyanide ions within same measurement method. To work on this site, a cost efficient dual responsive chemosensor, based on 1,8-naphthalimide and hydroxypyrones ring system with a hydrazone linker, has been synthesized in ethanol under ambient temperature conditions. Apparently, due to paramagnetic behavior, Cu^{2+} ions N,O-chelation with **4**, resulted in diminished ICT process and complete quenching of emission intensity. Besides, anions induced deprotonation elicit the internal charge transfer (ICT) and PET processes. In the present report, NMR titration experiments delineated the deprotonation based recognition mechanism. Sensor **4** loaded paper strip experimentation revealed the practical applicability via portable sensor kit for on-site detection of multi-analytes in aqueous medium. Additionally, it has been demonstrated that both deionized water and methanol assisted in selective discrimination of F^- and CN^- ions with **4**, in THF. Indeed, the fluorescent N,O-chelation successfully demonstrated that an efficient sensing probe has been synthesized under a green solvent like ethanol that can effectively detect multiple analytes generating instantaneous optical responses.

2. Experimental

2.1. Materials and instrumentations

4-Bromo-1,8-naphthalic anhydride, *n*-butylamine, 2-methoxyethanol, 3-acetyl-4-hydroxy-6-methyl-pyran-2-one hydrazine hydrate (80%), DMSO- d_6 and chloroform- d_1 were incurred from Sigma Aldrich. Tetrabutylammonium salts of different anions and metal perchlorates were bought from TCI chemicals and dried prior to use. Ethanol and THF employed for the synthesis or analysis were used as supplied without further purification. Water utilized in the analysis processes was obtained from Millipore system and deionized prior to use. Commercially available toothpaste (Colgate) and mineral water (Nestle) were purchased and analyzed for ions. All the metal ions and anions were incurred by the dissolution of their respective TBA salts in deionized water. Melting point was measured with the open capillary tube method using a GALLENKAMP variable heater melting point apparatus. ESI-Mass (negative mode) was calculated employing a microTOF-Q III instrument. UV-vis spectra were measured using a slit width of 1.0 nm and matched quartz cells on a Shimadzu UV-2600 UV-vis spectrophotometer. Fluorescence spectra and quantum yield (filter glass 2.5, dark offset) were recorded with a HORIBA Fluoro Max Plus Spectrofluorometer. ^1H and $^{13}\text{C}\{^1\text{H}\}$ NMR spectra were incurred on a Bruker 500 MHz spectrometry using TMS as an internal reference. NMR chemical shifts were reported in ppm and referenced to residual protonated solvent. Tetrabutylammonium

salts and metal perchlorates were used for anion and cation studies, respectively.

2.2. Preparations

2.2.1. Synthesis of 6-bromo-2-butyl-benzoisoquinoline-1,3-dione (**2**)

4-Bromo-1,8-naphthalic anhydride (0.277 g, 1 mmol) was dissolved in ethanol (20 mL). Later, *n*-butylamine (0.073 g, 1 mmol) was dropwise added to the ethanolic solution. The reaction mixture was refluxed with gentle stirring for 12 h, in an oil bath. The resulting mixture was allowed to cool to room temperature and concentrated under vacuum. The crude product was filtered down and washed 3–4 times by ethanol. Recrystallization of **2** in ethanol obtained a white crystalline solid. m.p. 103–104 °C. yield: 0.295 g (89%). ^1H NMR (400 MHz, CDCl_3 , 25 °C, TMS) δ (ppm): 8.63–8.61 (dd, 1H, ArH), 8.55–8.52 (dd, 1H, ArH), 8.39–8.37 (d, 1H, ArH), 8.02–8.00 (d, 1H, ArH), 7.83–7.79 (t, 1H, ArH), 4.16–4.12 (t, 2H, CH_2), 1.72–1.64 (m, 2H, CH_2), 1.46–1.36 (m, 2H, CH_2), 0.96–0.92 (t, 3H, CH_3) as shown in Fig. S1. $^{13}\text{C}\{^1\text{H}\}$ NMR (400 MHz, CDCl_3 , 25 °C, TMS) δ (ppm): 163.68 (C12), 163.66 (C1), 133.25 (C9/C3), 132.08 (C5), 131.27 (C8), 130.66 (C7), 130.26 (C4), 129.03 (C6), 128.17 (C2), 123.24 (C10), 122.38 (C11), 40.54 (C13), 30.32 (C14), 20.54 (C15), 14.01 (C16) as depicted in Fig. S2.

2.2.2. Synthesis of 2-butyl-6-hydrazinyl-benzoisoquinoline-1,3-dione (**3**)

Compound **2** (0.332 g, 1 mmol) was dissolved in 25 mL of ethanol followed by the addition of 80% hydrazine hydrate (0.3 mL, 3.3 mmol). The resulting solution was refluxed with stirring for 3 h in an oil bath. Finally, the precipitated orange colored crude product was collected under vacuum suction and washed with ethanol. Recrystallization of **3** was carried out in acetonitrile to obtain an orange crystalline solid. m.p. 220–223 °C. yield: 0.241 g (85%). ^1H NMR (400 MHz, CDCl_3 , 25 °C, TMS) δ (ppm): 9.10 (s, 1H, NH), 8.59–8.57 (d, 1H, ArH), 8.40–8.38 (d, 1H, ArH), 8.27–8.25 (d, 1H, ArH), 7.63–7.59 (t, 1H, ArH), 7.23–7.21 (d, 1H, ArH), 4.65 (s, 2H, NH_2), 4.01–3.97 (t, 2H, CH_2), 1.60–1.53 (m, 2H, CH_2), 1.36–1.27 (m, 2H, CH_2), 0.92–0.88 (t, 3H, CH_3) as shown in Fig. S3. $^{13}\text{C}\{^1\text{H}\}$ NMR (400 MHz, CDCl_3 , 25 °C, TMS) δ (ppm): 163.79 (C12), 162.94 (C1), 153.19 (C7), 134.22 (C9), 130.58 (C3), 129.30 (C5), 128.23 (C4), 124.13 (C2), 121.75 (C11), 118.45 (C6), 107.40 (C10), 104.01 (C8), 38.93 (C13), 29.86 (C14), 19.87 (C15), 13.77 (C16) as depicted in Fig. S4.

2.2.3. Synthesis of 2-butyl-6-(2-(1-(4-hydroxy-6-methyl-2-oxo-pyran-3-yl)-ethylidene)-hydrazinyl)-benzoisoquinoline-1,3-dione (**4**)

Compound **3** (0.283 g, 1 mmol) and 3-acetyl-4-hydroxy-6-methyl-pyran-2-one (0.168 g, 1 mmol) were added in ethanol (25 mL). The mixture was refluxed with continuous stirring at 100 °C. After refluxing for 12 h, the reaction mixture was left to cool at room temperature and concentrated under vacuum. The crude product was further purified by recrystallization with acetonitrile-hexane mixture (95:5) to give a novel compound **4** (0.345 g) as yellow crystalline solid. m.p. 253–254 °C. yield: 0.345 g (80%). ^1H NMR (400 MHz, CDCl_3 , 25 °C, TMS) δ (ppm): 15.52 (s, 1H, OH), 8.62–8.60 (d, 1H, ArH), 8.50–8.48 (d, 1H, ArH), 8.19–8.17 (d, 1H, ArH), 7.99 (s, 1H, NH), 7.74–7.70 (t, 1H, ArH), 7.13–7.11 (d, 1H, ArH), 5.89 (s, 1H, ArH), 4.15–4.11 (t, 2H, CH_2), 2.77 (s, 3H, $-\text{CH}_3$), 2.20 (s, 3H, $-\text{CH}_3$), 1.72–1.64 (m, 2H, CH_2), 1.46–1.36 (m, 2H, CH_2), 0.96–0.92 (t, 3H, $-\text{CH}_3$) as shown in Fig. S5. $^{13}\text{C}\{^1\text{H}\}$ NMR (400 MHz, CDCl_3 , 25 °C, TMS) δ (ppm): 178.62 (C17), 166.38 (C15), 164.39 (C14), 163.89 (C1/C12), 163.04 (C18), 144.78 (C7), 133.57 (C9), 131.68 (C3), 129.55 (C5), 126.40 (C4), 125.53 (C12), 123.74 (C11), 119.91 (C6), 115.59 (C10), 107.35 (C8), 104.30 (C16), 97.09 (C13), 40.42 (C19), 30.44 (C20), 20.61 (C23), 20.27 (C21), 15.99 (C22), 14.06 (C24) as depicted in Fig. S6. HRMS (ESI): $[\text{M} - \text{H}]^-$ calcd for $[\text{C}_{24}\text{H}_{22}\text{N}_3\text{O}_5]^-$, m/z 432.1559; found m/z 432.1583 (Fig. S7).

2.3. General spectroscopic procedures

2.3.1. UV-vis and fluorometric measurements of **4** with Cu^{2+}

Stock solution of **4** (2×10^{-5} M) in THF (10 mL) & perchlorate salts of metal ions (4×10^{-4} M) in deionized water (5 mL) were prepared. UV-vis spectrometric study involved sequential addition of 20–300 μL of Cu^{2+} ions into the solution of **4** (2 mL) in a cuvette. On the other side, fluorometric study involved the gradual addition of 20–500 μL of Cu^{2+} ions into the solution of **4** (2 mL) in a cuvette. The obtained solutions were stirred for 1 min and UV-vis/fluorometric spectra were collected at room temperature by adjusting slit width parameters to 2/2 nm and 5/5 nm, respectively.

2.3.2. Job plot measurements

Stock solutions of sensor **4** (10^{-4} M) in THF (10 mL) & $\text{Cu}(\text{ClO}_4)_2$ (10^{-4} M) in deionized H_2O (10 mL) were prepared. A solution of sensor **4** in varying amounts i.e. 0.5, 0.45, 0.40, 0.35, 0.30, 0.25, 0.20, 0.15, 0.10, 0.05 and 0 mL were transferred to individual volumetric flasks (5 mL). Later, Cu^{2+} solution, 0, 0.05, 0.10, 0.15, 0.20, 0.25, 0.30, 0.35, 0.40, 0.45 and 0.5 mL, was added to a solution of sensor **4** separately. Finally, each flask was made up to 5 mL with THF. Then, individual flask solution was immixed for 1 min and transferred to fluorescence cuvette (2 mL). All the fluorescence spectra were recorded at room temperature.

2.3.3. UV-vis and fluorometric measurements of **4** with F^-/CN^-

Stock solution of **4** (2×10^{-5} M) in THF (10 mL) & TBA salts of anions (4×10^{-4} M) in deionized water (5 mL) were prepared. UV-vis spectrometric study involves sequential addition of 5–120 μL of F^- /20–400 μL of CN^- ions into the solution of **4** (2 mL) in a cuvette. On the other side, fluorometric study involve the gradual addition of 5–150 μL of F^- /10–400 μL of CN^- ions into the solution of **4** (2 mL) in a cuvette. The incurred solutions were stirred for 1 min, prior to recording UV-vis/fluorometric spectra at room temperature, using slit width of 2/2 nm and 5/5 nm respectively.

2.3.4. Job plot measurements

Stock solutions of sensor **4** (10^{-4} M) in THF (10 mL) & TBA-X (X- F^- and CN^-) salts (10^{-4} M) in deionized H_2O (10 mL) were prepared. Different volumes of sensor **4** i.e. 0.5, 0.45, 0.40, 0.35, 0.30, 0.25, 0.20, 0.15, 0.10, 0.05 and 0 mL were measured and transferred to volumetric flasks of 5 mL capacity. Additionally, 0, 0.05, 0.10, 0.15, 0.20, 0.25, 0.30, 0.35, 0.40, 0.45 and 0.5 mL of the F^-/CN^- solution were added to above solution separately. Finally, every flask was filled up to 5 mL mark with THF. Then, individual solutions were mixed thoroughly for 1 min and later pipette out (2 mL) to fluorescence cuvette. Fluorescence spectra were obtained at room temperature.

2.3.5. Competitive experiments

Stock solution of **4** (2×10^{-5} M) in THF (10 mL) & perchlorate salts of metal ions (4×10^{-4} M)/TBA salts of anions (4×10^{-4} M) in deionized water (5 mL) were prepared. Fluorometric competitive study involved initial addition of 100 μL of relevant anions/200 μL of metal ions to the solution of **4** (2 mL) in a cuvette, followed by the addition of 100 μL of F^- or CN^- /200 μL of Cu^{2+} ions, respectively. After stirring the solutions for 1 min, emission spectra were recorded employing a slit width of 5/5 nm.

3. Result and discussions

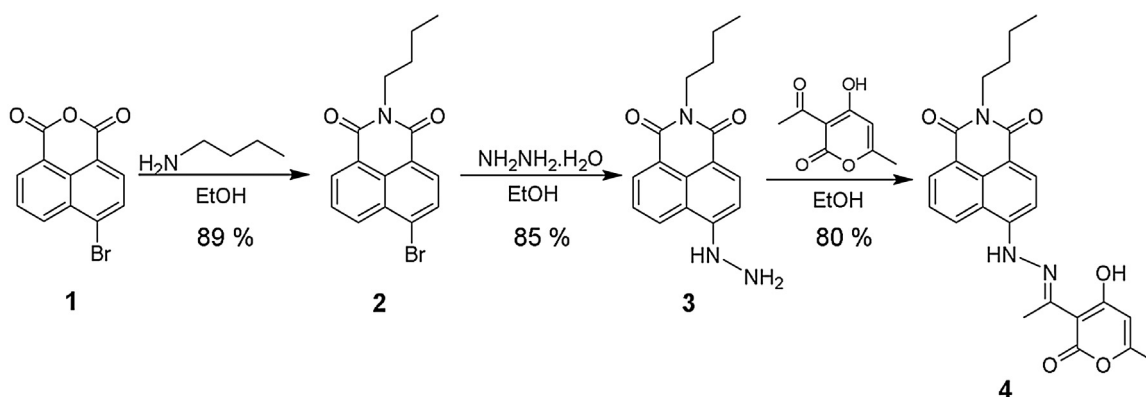
3.1. Synthesis methodology of **4**

Initially, two reactive precursor compounds i.e. 6-bromo-2-butyl-benzoisoquinoline-1,3-dione (**2**) and 2-butyl-6-hydrazinyl-benzoisoquinoline-1,3-dione (**3**), have been consecutively synthesized employing ethanol as reaction medium [42–45]. Later condensation reaction between compound **3** and 3-acetyl-4-hydroxy-6-methyl-pyran-2-one in 1:1 ratio in ethanol for 12 h results in the formation of deep yellow solution of novel hydrazone Schiff's base product (80% yield) i.e. 2-butyl-6-(2-(1-(4-hydroxy-6-methyl-2-oxo-pyran-3-yl)ethylidene)hydrazinyl)-benzoisoquinoline-1,3-dione (**4**), as shown in Scheme 1. Ambient temperature conditions were used to conclude the condensation reaction. Further isolation of the pure compounds were achieved through recrystallization in pure ethanol rather than tedious column chromatography. The detailed experimental procedures and the characterizations of **4** are described in above.

3.2. Colorimetric responses of **4** with Cu^{2+}

The changes observed in the absorption spectral pattern of **4** with the addition of different metal ions in THF/ H_2O are shown in Fig. 1. It is inferred from the absorbance plots that with the addition of 2 equiv. of different metal ions (except for Cu^{2+}), the absorption band at 412 nm undergoes slightly red shift (8 nm), with a minor change in the absorption intensity. Contrary to this, with the addition of Cu^{2+} (2 equiv.) to the solution of **4**, the ICT absorption band at 412 nm was completely vanished and solution color changed from yellow to colorless (Fig. 1 Inset). This in turn pointed out that chelation of Cu^{2+} ions with **4** ensued in reduced electron density, leading to diminished ICT process [46]. Hence, sensor **4** showed high selectivity towards Cu^{2+} ions over other common metal ions.

To obtain further insight into the binding characteristics of Cu^{2+} with **4**, spectrophotometric titration experiments were conducted with Cu^{2+} ions in aqueous-organic solution. Upon sequential



Scheme 1. Synthetic approach to prepare the hydrazone Schiff base of chemosensor **4** derived from 1,8-naphthalimide and dehydroacetic acid.

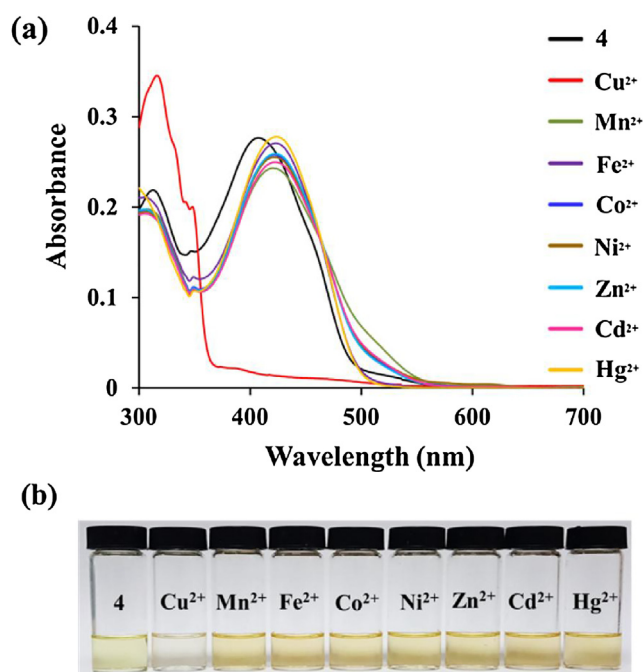


Fig. 1. Absorbance spectra (a) of **4** (2×10^{-5} M) with the compartment of 2 equiv. of different metal ions in THF/H₂O; (b) Inset: changes in the color observed (bottom) with the addition of different metal ions (2 equiv.) to the solution of **4** (2×10^{-5} M) solution in ambient light.

accession of Cu²⁺ to a solution of **4**, the ICT absorption band at 412 nm undergoes a slight bathochromic shift (3 nm) with a simultaneous uninterrupted decrease in the absorbance intensity, that halts at 3 equiv. of Cu²⁺ ions (Fig. 2). A clear isosbestic point was indicated at 355 nm ascertaining the existence of equilibrium between the two species i.e. **4** and **4** + Cu²⁺, during the titration experiment. As a result, yellow solution of **4** slowly changed to colorless solution (Fig. 2 Inset).

3.3. Colorimetric responses of **4** with F⁻ and CN⁻

To investigate the colorimetric response patterns of **4** (2×10^{-5} M in THF) with anions, the UV–vis absorbance experiments were conducted with tetrabutylammonium salts (TBA–X; X = F⁻, Cl⁻, Br⁻, I⁻, CN⁻, SCN⁻, AcO⁻, ClO₄⁻, HSO₄⁻, H₂PO₄⁻, NO₂⁻,

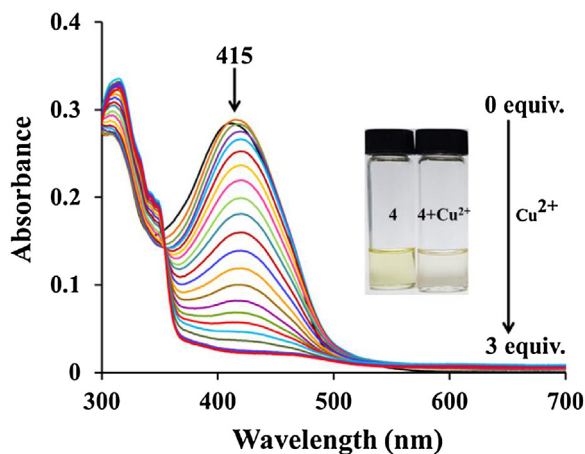


Fig. 2. Absorbance titration spectra of **4** (2×10^{-5} M) with various concentrations of Cu²⁺ (0–3 equiv.) in THF/H₂O; Inset: the color of **4** (left) and **4** + Cu²⁺ (right) upon the addition of 3 equiv. of Cu²⁺.

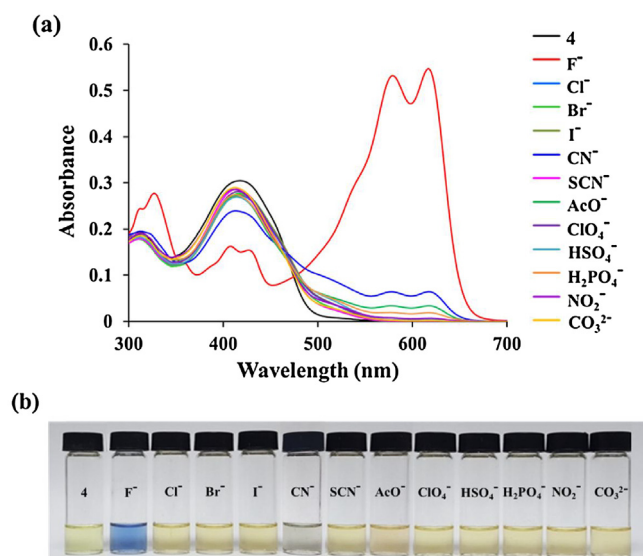


Fig. 3. Absorbance spectra (a) of **4** (2×10^{-5} M) with the addition of 1 equiv. of different anions in THF/H₂O; (b) Inset: color change noticed (bottom) in sensor **4** (2×10^{-5} M) solution with anions (1 equiv.).

CO₃²⁻) of various anions, (Fig. 3). Visual inspection of **4** solution, before and after the addition of anions displayed noticeable color changes only with F⁻ and CN⁻ ions, which confirmed existence of strong interaction exist between **4** and F⁻/CN⁻ ions. Additionally, compartment of the OH group in vicinity of hydrazone group offered additional interaction site for F⁻ and CN⁻ ions. On the other hand, the addition of other anions to the solution of **4** did not bring on any appreciable color changes. Also, absorption spectrum of **4** showed absorbance maxima at 412 nm due to intra-molecular charge transfer phenomenon (ICT) i.e. n → π* transitions [15]. Addition of 1 equiv. of various anions (except for F⁻ and CN⁻ ions), the absorption spectra of **4** did not display any substantial change with minor fluctuation in absorbance intensity at 412 nm. However, with F⁻ ions (1 equiv.), the ICT absorption band at 412 nm (1.6×10^4 L mol⁻¹ cm⁻¹) underwent a drastic decrease and ultimately split up into two adjacent bands positioned at 408 nm and 428 nm. Simultaneously, two new absorption maxima at 580 nm and 620 nm, with prominent bathochromic shift (172 nm and 192 nm respectively), were observed as depicted in Fig. 3. This leads to visible naked eye color change of solution **4** from yellow to blue in ambient light; Fig. 3 Inset. Similarly, addition of CN⁻ ions (1 equiv.) to the solution **4**, ensued in two new bands at 581 nm and 622 nm with diminished 412 nm band. Herein, the solution color shows perceptible changes from yellow to violet. These remarked changes in the absorption spectra with F⁻/CN⁻ ions were due to the deprotonation and subsequent ameliorated electron donor propensity of N-/O- moiety, within the receptor molecule, resulting in heightened ICT process [46,47]. Thus, **4** emerged as a relevant probe for naked-eye recognition of F⁻ and CN⁻ ions, with noticeably chromogenic changes, in aqueous-organic medium.

UV–vis titration experiments were carried out to determine the sensitivities of **4** toward F⁻ and CN⁻ ions. As shown in Fig. S8(a), following spectroscopic changes observed when a solution of **4** in THF were treated with increasing quantities of TBAF solution in deionized water. Upon sequential addition of TBAF to **4**, the band at 412 nm progressively decreased, whereas two new bands with peak positions at 580 nm and 620 nm displayed a gradual increase and attained its maximum absorbance intensity at 1.2 equiv. of F⁻ ions. The yellow solution of **4** slowly changed to blue color solution, Fig. S8(a) Inset. An isosbestic point at 480 nm further ensured that equilibrium exists between **4** and **4** + F⁻ species, during the course

of the titration. As demonstrated in Fig. S8(b), addition of TBACN to **4**, also displayed a similar pattern as that of F^- with a decrease in band at 412 nm and simultaneously increases in two new bands positioned at 581 nm and 622 nm. Herein, an isosbestic point was observed at 482 nm affirming existence of equilibrium between **4** and $4 + CN^-$ species. The solution color slowly changes from yellow to violet with the incremental addition of 0–3.5 equiv. of CN^- , Fig. S8(b) Inset. Therefore, it was reasoned out that F^- or CN^- ions, induced deprotonation of O–H and N–H moieties, resulting in the prolonged conjugation in **4**. Due to meliorated electronic delocalization, the energy required for $p-p$ transitions scale down, ensuing two new absorption bands at around 580 nm and 620 nm.

3.4. Fluorometric responses of **4** with Cu^{2+}

The emission intensity changes observed in the spectra of **4** induced by cations, such as Cu^{2+} , Mn^{2+} , Fe^{2+} , Co^{2+} , Ni^{2+} , Zn^{2+} , Cd^{2+} , Hg^{2+} are shown in Fig. 4. Addition of Cu^{2+} ions to the solution of **4** ensued a sudden sharp decrease in the emission intensity at 520 nm compared to other competitive metal ions. The fluorescence color changed from bright green to dull blue with Cu^{2+} ions only (Fig. 4 Inset). It was interpreted that complete quenching of emission intensity was observed as a consequence of paramagnetic behavior of Cu^{2+} ions [46].

To work out the detection range and correlation between fluorescence responses of sensor **4** at 520 nm and Cu^{2+} ion concentration, fluorescence titration experiments were performed. It was remarked that incremental addition of Cu^{2+} (0–5 equiv.) to a solution of **4**, results in consistent decreases in emission intensity at 520 nm with a slightly bathochromic shift (10 nm), as depicted in Fig. 5. The solution color changed from yellow to colorless in Cu^{2+} , with the fluorescence color change from bright green to dull blue (Fig. 5 Inset). Further, detection limits were calculated based on fluorometric titration results observed at

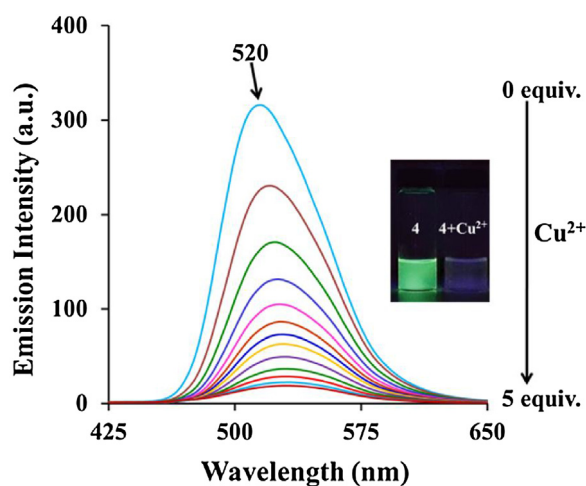


Fig. 5. Emission titration spectrum of **4** (2×10^{-5} M) in the presence of incremental concentrations of Cu^{2+} ions (0–5 equiv.) in THF/ H_2O ; Inset: the color of **4** (left) and **4** + Cu^{2+} (right) with 5 equiv. of Cu^{2+} ions.

maximum wavelength, employing formulation $3\sigma/C$; where, σ corresponds to the standard deviation of the blank and C is the slope of each titration curve and found to be 0.962 ppm.

Further, competitive experiments were carried out to establish the selectivity of **4** toward Cu^{2+} ions. As shown in Fig. 6, sensor **4** was treated 2 equiv. of Cu^{2+} in the presence of other metal ions (Mn^{2+} , Fe^{2+} , Co^{2+} , Ni^{2+} , Zn^{2+} , Cd^{2+} , Hg^{2+}) of the same concentration. The fluorescence quenching pattern obtained evidently ensued that other common competing metal ions have relatively negligible interference.

Job's plot was delineated based on the fluorescence intensity of **4** at 530 nm, against the molar fraction of **4**, maintaining the constant total concentration, to obtain the binding ratio between **4** and Cu^{2+} . The maxima was attained when the molar fraction of **4** / [**4** + (Cu^{2+})], was 0.67, indicating that the stoichiometric ratio of **4** with Cu^{2+} to be 2:1 Fig. S9(a). As interaction of **4** with Cu^{2+} ions, resulted in drastic change in the emission intensity therefore emission titration experiments were employed to calculate the association constant and quenching constant. Association constant were calculated according to the Benesi–Hildebrand equation as follows:

$$1/(I - I_0) = 1/\{K(I_{max} - I_0)[Ion]^n\} + 1/[I_{max} - I_0]$$

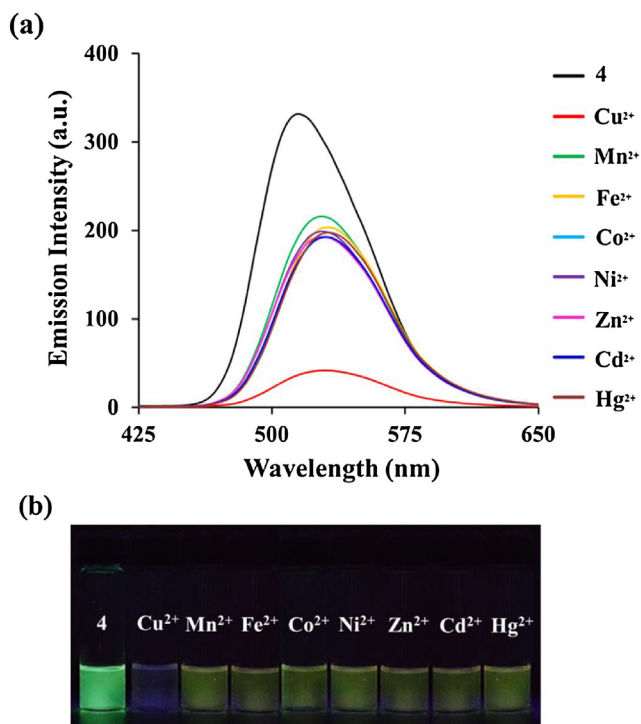


Fig. 4. Emission spectral pattern (a) of **4** (2×10^{-5} M) obtained with the addition of 2 equiv. of different metal ions in THF/ H_2O ; (b) Inset: color change observed (bottom) upon the addition of different metal ions (2 equiv.) to the sensor **4** (2×10^{-5} M) solution, under the UV-lamp (365 nm).

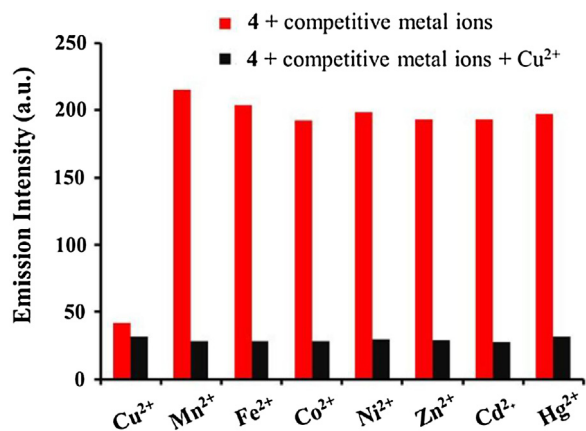


Fig. 6. Relative emission intensity bar graph showing competitive selectivity of **4** (2×10^{-5} M) toward Cu^{2+} (2 equiv.) in the presence of other competing metal ions (2 equiv.) in THF/ H_2O .

I_0 relates to the fluorescence of **4** without any ion, I is the fluorescence recorded with ion, I_{\max} corresponds to the fluorescence in the presence of added $[Ion]_{\max}$ and K is the association constant, which was calculated from the slope of the straight line of the B-H plot of $1/(I - I_0)$ against $1/[Ion]^n$. The association constant value of **4** with Cu^{2+} was determined from the emission intensity plots measured at 530 nm. The association constant (K_a) of **4** with Cu^{2+} was calculated to be $1.26 \times 10^5 \text{ L mol}^{-1}$, Fig. S10(a). Moreover, to elucidate the quenching phenomenon in **4** with Cu^{2+} ions, the Stern-Volmer (S-V) plot, a graph was plotted between intensity ratio, I_0/I and concentration of Cu^{2+} ions as shown in Fig. S11(a). The slope of the obtained straight line (R^2 0.9765 for Cu^{2+}) rendered the quenching constant, $K_{S-V} 2.04 \times 10^5 \text{ mol L}^{-1}$ for Cu^{2+} . This deciphered that quenching of emission intensity in the interactive ground state $\mathbf{4} + Cu^{2+}$, was the entirely active process [47,48]. Additionally, noticeable decrease in the quantum yield value of **4** from 4.24 to 1.54; in Fig. S12(a) was obtained. Thus, detectable fluorescence quenching was observed only with Cu^{2+} ions compared to all other metal ions.

3.5. Fluorometric responses of **4** with F^- and CN^-

Next, to further examine the dual-mode recognition behavior of **4** toward anions, the fluorometric experiments were performed at an excitation wavelength of 412 nm, under ambient conditions. Initially, the fluorescence spectra were recorded in the presence of various anions (F^- , Cl^- , Br^- , I^- , CN^- , SCN^- , AcO^- , ClO_4^- , HSO_4^- , $H_2PO_4^-$, NO_2^- , CO_3^{2-}) as shown in Fig. 7 and the results show that the fluorescence of **4** was quenched significantly only with F^- and CN^- ions, with a minor bathochromic shift (5 nm). Anion induced deprotonation of N–H and O–H groups at the receptor site, facilitate lone pair of nitrogen/oxygen for heightened PET process [46], leading to quenching of emission intensity.

Fluorometric titration experiments were also conducted to investigate parameters such as detection limit and the results obtained are shown in Fig. S13(a). A consistent decline with a slightly bathochromic shift (5 nm) in the emission intensity at 515 nm was observed for **4**, when the F^- concentration increased from 0–1.5 equiv. The solution color changed from bright yellow to

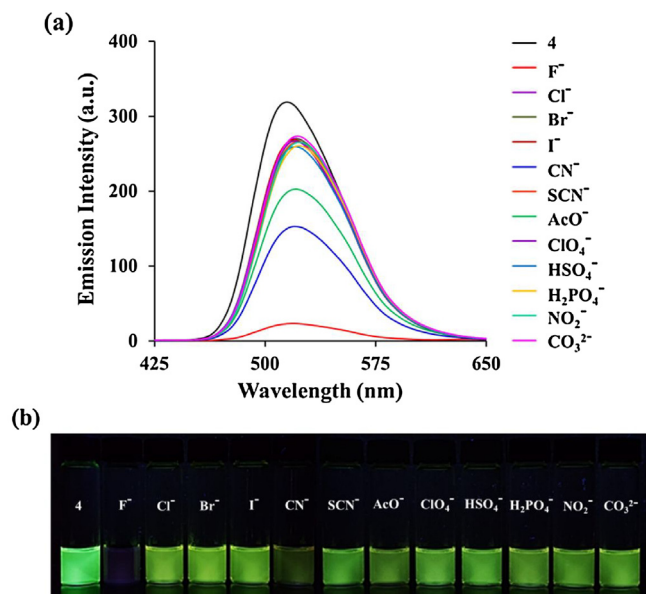


Fig. 7. Emission spectra (a) of **4** ($2 \times 10^{-5} \text{ M}$) with the addition of 1 equiv. of various anions in THF/ H_2O solution; (b) Inset: color change observed (bottom) upon the addition of various anions (1 equiv.) to the sensor **4** ($2 \times 10^{-5} \text{ M}$) solution, under UV-lamp (365 nm).

deep blue in F^- with the fluorescence color change from bright green to dark, Fig. S13(a) Inset. The detection limit was found to be 0.023 ppm. These results were further ascertained through decreased quantum yield value from 4.24 to 1.41 with F^- (1 equiv.) as shown in Fig. S12(b). Further, **4** solution was titrated with CN^- ions and it was observed that the sequential addition of 0–3.5 equiv. of CN^- ions, resulted in consistent decrement in the emission intensity at 519 nm with a slightly red shift of 8 nm, with fluorescence color changes from bright green to dull green, Fig. S13 (b) & Inset. The detection limit was calculated to be 0.073 ppm. Quantum yield value of **4** dropped down to 1.59 with CN^- (1 equiv.); Fig. S12(c).

In order to ascertain the selectivity of **4** toward recognition of F^-/CN^- ions, competitive experiments with 1 equiv. of F^- and 1 equiv. of other common competitive anions (Cl^- , Br^- , I^- , SCN^- , AcO^- , ClO_4^- , HSO_4^- , $H_2PO_4^-$, NO_2^- , CO_3^{2-}) were performed. It was observed that the fluorescence intensity of **4** with F^- was not significantly interfered even in the presence of competing anions Fig. 8(a). The fluorescence quenching observed with F^- was not affected with all of the competing anions together. Similar fluorescence experiments were carried out to confirm the selective nature of **4** toward CN^- ions in the presence of other anions. Addition of 1 equiv. of CN^- to a solution of **4**, in the presence of relevant anions (1 equiv.), still quenched the fluorescence affirming that competitive anions have negligible interference in the recognition of CN^- ions; Fig. 8(b). These results revealed the high selectivity of **4** for the recognition of F^-/CN^- ions.

Continuous variation methodology was followed to determine the fluorogenic quantitative sensing ability of **4** toward F^-/CN^- ions. As deduced from the Job's plot of **4** with F^- and CN^- anions, the maxima was achieved when the molar fractions of (**4**)/

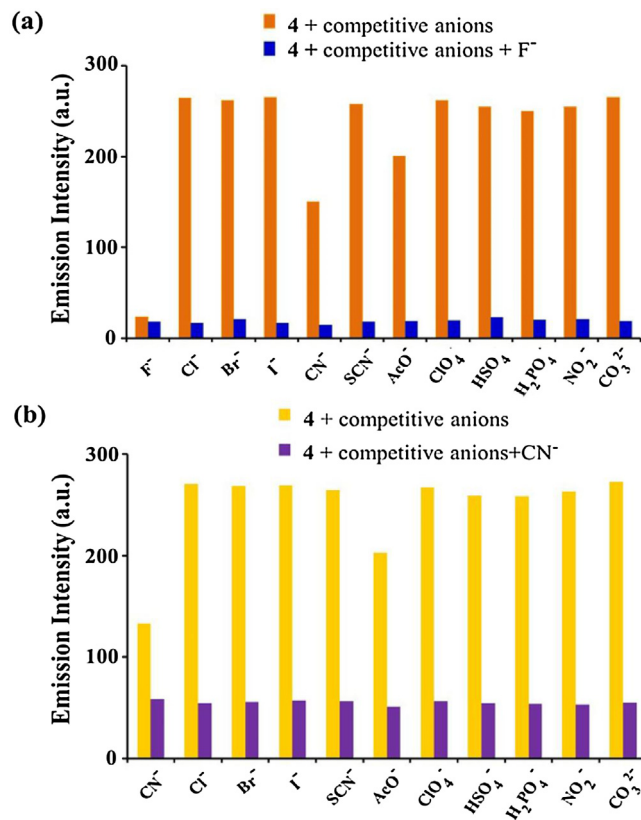


Fig. 8. Relative emission intensity bar graphs showing competitive selectivity of **4** ($2 \times 10^{-5} \text{ M}$) toward (a) F^- (1 equiv.) and (b) CN^- (1 equiv.) in the presence of competing anions (1 equiv.).

$[(4)+(F^-)]$ and $(4)/[(4)+(CN^-)]$, were 0.69 and 0.5 respectively, indicating that the ratios of **4** with F^- (2:1) and CN^- (1:1) were achieved in Fig. S9(b) and (c). The association constant (K_a) of **4** with F^- and CN^- was calculated to be $1.5 \times 10^5 \text{ L mol}^{-1}$ and $0.62 \times 10^5 \text{ L mol}^{-1}$, respectively, using the Benesi–Hildebrand equation, Fig. S10(b) and (c). From the association constant values, it is interpreted that the F^- has the higher fluorescence binding affinity compared with CN^- towards **4**. The detection limit of **4** was found to be $1.2 \times 10^{-6} \text{ M}$ for F^- and $2.79 \times 10^{-6} \text{ M}$ for CN^- . An almost straight line (R^2 0.9879/0.9864 for F^-/CN^-) with quenching constants, K_{S-V} : $3.54 \times 10^5 \text{ molL}^{-1}/2.41 \times 10^5 \text{ molL}^{-1}$ for F^-/CN^- , respectively; Fig. S11(b) and (c), further support the enhanced PET process.

3.6. Mechanism of interaction of **4** with ions

In order to elucidate the bonding interaction of Cu^{2+} ions with **4**, NMR titration experiments were performed, in $DMSO-d_6$ as shown in Fig. S14. Initially, sequential addition of Cu^{2+} ions (0–5 equiv.) to the **4**, resulted into complete disappearance of O–H (δ 15.51 ppm) proton signal. Additionally, aliphatic protons in vicinity of hydrazone group and other aromatic ring protons undergoing upfield shift, a redistribution of electric charge on the naphthalimide rings was encountered upon interaction with Cu^{2+} ion [49,50]. These observations clearly indicated that two sensor molecules encircled the Cu^{2+} ions copper ions in a square planar geometry, with N/O atoms of hydrazone/hydroxy groups, respectively, as interacting sites [46,51,52] Interpretation of the experiment data affirmed the proposed mechanism and related 2:1 stoichiometry.

Further to gain insight into the sensing mode of **4** toward F^-/CN^- ions, NMR titration experiments were performed in $CDCl_3$ and

changes observed in the 1H NMR spectra were depicted in Fig. 9. Initially, F^- ions (0–1 equiv.) were gradually added to **4** and corresponding spectra were analyzed. It was noticed that with the addition of 0.2 equiv. of F^- to **4**, the resonance signal related to O–H and N–H proton at δ 15.51 ppm/7.99 ppm vanished completely; Fig. 9(a). Thus, it was concluded that F^- ions interacted with **4** through deprotonation of N–H and O–H moieties [50,52,53]. Beside this, other aromatic ring protons also displayed prominent up-field chemical shifts. These chemical shifts were encountered as a consequence of deprotonation, which resulted in increased electron density leading to enhanced ICT process within the receptor molecule [54,55]. Later, with the addition of 1 equiv. of F^- ions, a very weak signal appeared at 16.51 ppm, which affirmed the existence of $[FHF]^-$ dimer species [56]. This dimer formation further supports that deprotonation took place upon interaction of **4** with F^- ions. These results confirmed that F^- ions interact with hydrazone as well as hydroxyl group protons, as shown in Fig. 9(a) Inset.

Moreover, similar interaction mechanism between **4** and CN^- ions was concluded from the NMR titration experiment. Different equivalents (0–1 equiv.) of TBACN were sequentially added to the solution of **4** in $CDCl_3$ and the observed 1H NMR spectra were shown in Fig. 9(b). When 0.2 equiv. CN^- was added, the signal existing for the proton of O–H and N–H groups at 15.51 ppm/7.99 ppm disappeared immediately, which evidently showed that deprotonation occur instantaneously [54,55]. The other aromatic protons resonance signals undergoes a gradual upfield shift due to the shielding effect. Based on the analysis and interpretation of 1H NMR titration spectra, we proposed a potential mechanism for the interaction between receptor **4** and CN^- as depicted in Fig. 9(b) Inset. Thus, **4** behaves as a highly sensitive chemosensor for both F^- and CN^- ions in aqueous-organic medium.

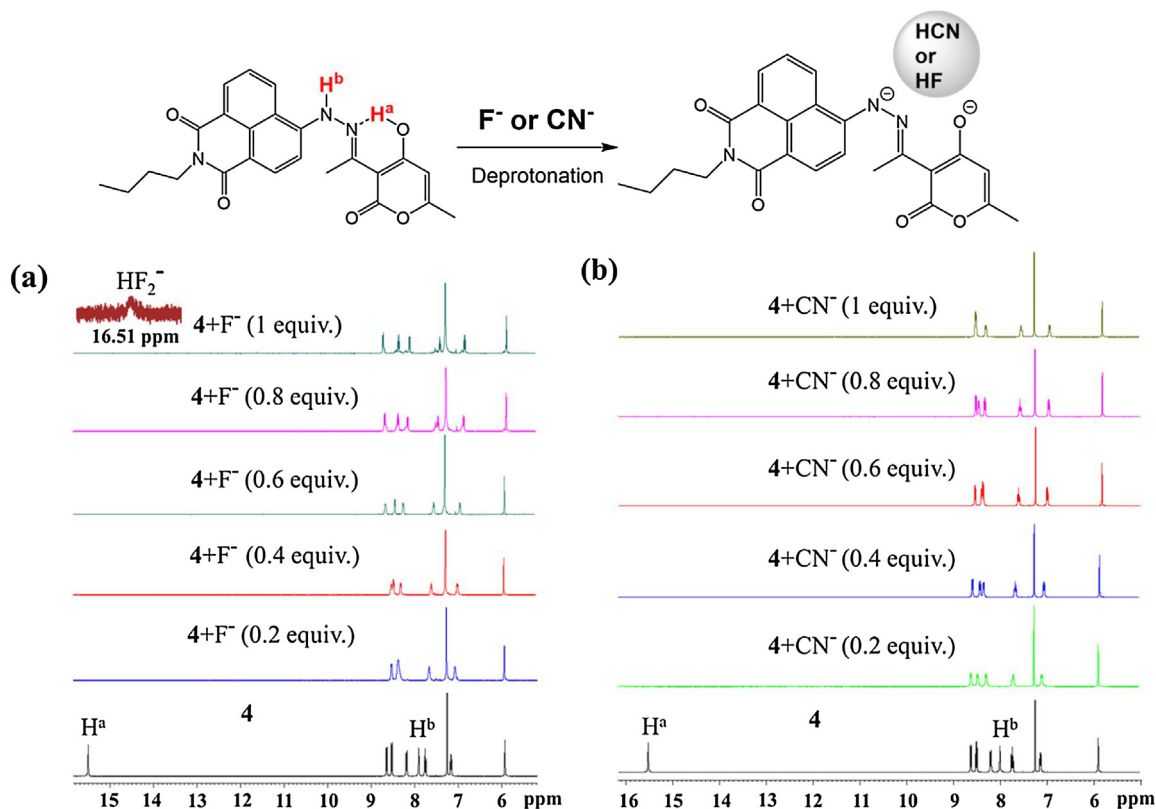


Fig. 9. 1H NMR titration plot of **4** with (a) F^- (0–1 equiv.) and (b) CN^- (0–1 equiv.) in $CDCl_3$. Inset: Deprotonation phenomenon in **4**, with F^-/CN^- ions.

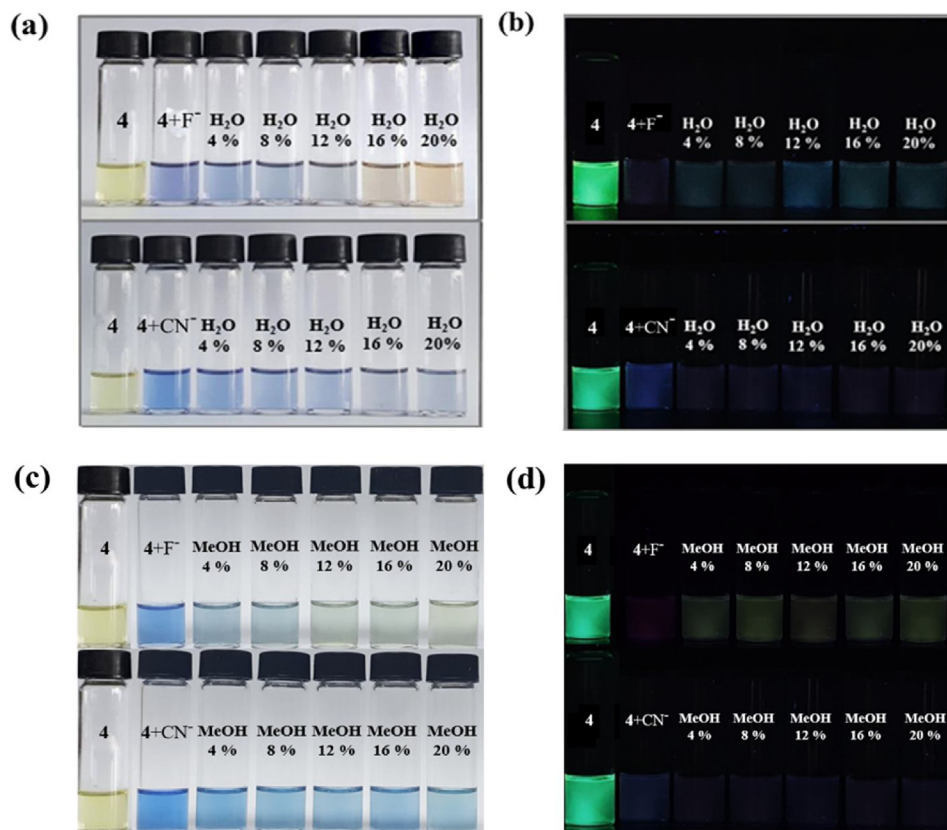


Fig. 10. Photographs of **4** (10^{-3} M) with F^- and CN^- ions (4×10^{-4} M) in THF solution, under ambient light/UV lamp with (a)/(b) H_2O (0–5 equiv.) and (c)/(d) MeOH (0–5 equiv.), respectively.

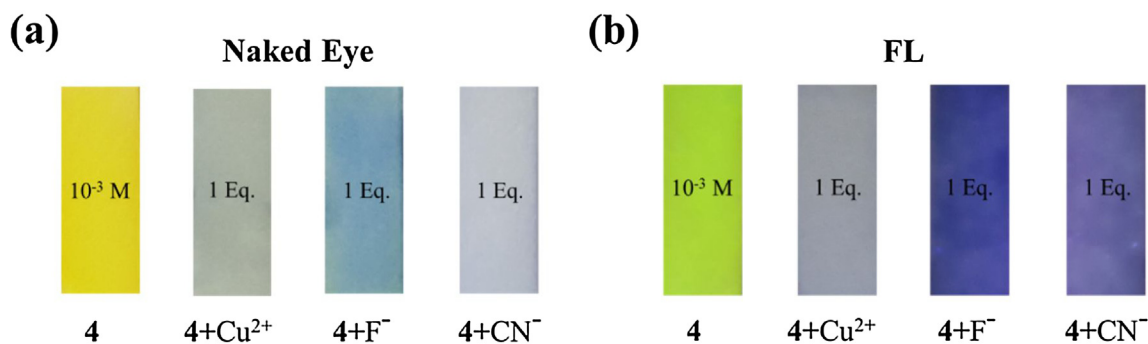


Fig. 11. Photographs of paper strips of **4** (10^{-3} M) with Cu^{2+} , F^- and CN^- ions (4×10^{-4} M) in THF/ H_2O solution under (a) ambient (b) UV radiation.

3.7. Discrimination with deionized water/methanol

Both colorimetric and fluorometric spectral patterns undergo a significant change with the addition of deionized water to the **4** + F^- /**4** + CN^- THF solution. During the colorimetric experiments, successive addition of deionized water (5 equiv.) to the **4** + F^- solution, ensued in visible naked eye color change from blue to orange Fig. 10(a). As plotted in Fig. S15(a), following colorimetric changes were observed as a result of drastic decrease in the absorption intensity of bands at 580/581 nm and 620/622 nm. In contrast only, slight change in the intensity of blue color was observed in **4** + CN^- solution. However, during the fluorometric experimentation, Fig. S16(a), addition of F^- ions (1 equiv.) to **4** solution, resulted in complete quenching of the emission intensity, but gradual addition of deionized water (0–5 equiv.) to this

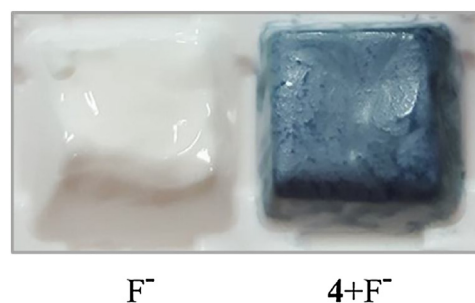


Fig. 12. Photographs of visible naked eye color of commercial toothpaste (NaF, 20 mg/kg); white and with **4** (10^{-3} M) in THF; blue, under ambient light. (For interpretation of the references to colour in this figure legend, the reader is referred to the web version of this article.)

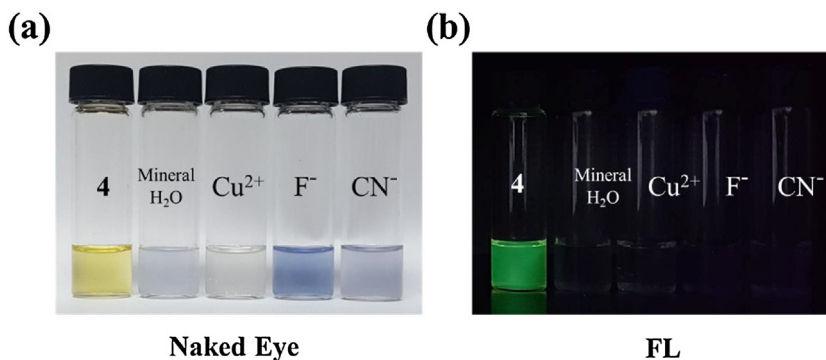


Fig. 13. Photographs of fluoridated mineral water (F^- , 0.5 mg/L) with **4** (2×10^{-5} M) in the presence of Cu^{2+} , F^- and CN^- ions (1.5, 0.07 (less than 0.08) and 2 mg/L, WHO permissible limits) under (a) ambient (b) UV radiation.

solution, again leads to the enhancement in emission intensity. On the other side, minimum emission intensity was observed with the addition of CN^- (3 equiv.) to a solution of **4**. Later, sequential addition of deionized water (0–5 equiv.) to the **4** + CN^- solution, resulted in thorough quenching of the emission intensity Fig. 10(b). Similar colorimetric and fluorometric experiments shown in Figs. S15(b) and S16(b), were performed with methanol. Addition of methanol (0–5 equiv.) to **4** + F^- solution, resulted in visible naked eye color change from blue to grey as shown in Fig. 10(c). However, no detectable color change was observed in **4** + CN^- solution. Interpretation of fluorometric results revealed that of **4** + F^- solution showed slight increase in emission intensity from completely quenched state. Contrary to this, residual fluorescence of **4** + CN^- solution undergoes complete quenching, Fig. 10(d). Since F^- ions exhibits high hydration energy and strong electronegativity [19], as a result significant solvent competitiveness exists, ensuing in reduced interaction between **4** and F^- ions. As a consequence, in the presence of deionized water/methanol, intra-molecular charge transfer (ICT) process gets diminished, contributing to visible naked eye color changes. However, PET process become more favorable leading to slight restoration of fluorescence [46]. Hence, deionized water or methanol could be used for the colorimetric as well as fluorometric discrimination of the two anions in organic medium.

4. Practical applications

4.1. Paper strips experiments

To ascertain the solid-state sensing ability of **4**, sensor loaded paper strips (Whatman filter paper no.1) were developed for the real-time analysis of Cu^{2+} , F^- and CN^- ions in aqueous medium. Initially, filter papers (3×1 cm²) were plunged with **4** (10^{-3} M) solution for about 5 mins and then dried off completely. Later, aqueous solution of Cu^{2+} ions were added on the loaded paper strips, the color of the paper strip changed immediately from yellow to colorless under ambient light as shown in Fig. 11(a). Similarly, with F^- and CN^- ions in water solution, the color changed from yellow to dark blue/gray, respectively. Under UV lamp ($\lambda_{ex} = 412$ nm), an apparent color change of **4** from bright green to dark occurred immediately, Fig. 11(b). The observed color changes were due to the deprotonation phenomenon observed in **4** with $Cu^{2+}/F^-/CN^-$ ions. Thus, sensor **4** has demonstrated both naked eye color and fluorometric recognition efficiency for metal ion as well as anions in the solid phase. Competitive metal ions and anions have not posed any interference during the paper strip experimentation. Hence, sensor **4** loaded paper strips can be conveniently used for the recognition of $Cu^{2+}/F^-/CN^-$ ions, without any additional equipmentation.

4.2. Real samples analysis

As established earlier, sensor **4** responds selectively for fluoride ions in solid state as well. In order to validate solid state applicability in practical samples, commercially available products such as toothpaste were analyzed for fluoride ion contents. A gram of toothpaste was treated with **4** (10^{-3} M, 400 μ L), sample color changes immediately from white to blue, ascertaining the presence of fluoride ions (20 ppm) as shown in Fig. 12.

Further, Cu^{2+} as well as F^-/CN^- ions were analyzed in fluoridated mineral water to corroborate competitive selectivity. Commercially available fluoridated mineral water (F^- , 0.5 mg/L) was supplemented with Cu^{2+} (2 mg/L), F^- (1.5 mg/L) and CN^- (0.07 mg/L) ions. Detectable ions solutions (1 mL) were treated separately with **4** (1 equiv. for Cu^{2+} and F^- , 15 equiv. for CN^-) in the presence of major constituent of mineral water such as Na^+ , Mg^{2+} , Ca^{2+} salts. Prominent visible naked eye color changes from yellow to colorless (Cu^{2+}) and blue (F^-/CN^-) was observed as shown in Fig. 13(a). Additionally, emission intensity undergoes completely quenching, depicted in Fig. 13(b). Thus, it has been successfully established that **4** displayed high competitive selectivity for ions in commercial commodities within WHO defined limits.

5. Conclusions

In ratiocination, a novel dehydroacetic acid based hydrazone Schiff's base sensor from three-step and high-yield syntheses under green approach like ethanol solvent has been prepared that exhibited high sensitivity and selectivity for Cu^{2+} , F^- and CN^- ions, within WHO accentuated detection limits. The presence of two receptor sites in a molecular sensor revealed instantaneous optical responses with ions. Sensor possessing N,O chelation with Cu^{2+} ions accounted for reduced ICT process, resulting in disappearance of absorption band at 412 nm. This brought on yellow color solution to colorless. However, with F^- and CN^- ions, two new absorption bands at 580/620 nm and 581/622 nm, imparting blue/violet color to the solution, respectively, were observed. As anions induced deprotonation resulted in enhanced ICT within the molecules. Emission intensity was substantially quenched in the presence of detectable metal ions as well as anions, due to inherent paramagnetism and enhanced PET process, respectively. Competitive experiments result further uncovered that common competing ions had negligible effect on the selective sensing of Cu^{2+} , F^- and CN^- ions, under ambient conditions. Deprotonation phenomenon of N–H and O–H moieties in the presence of ions was ascertained through ¹H NMR titration experiments. Job's plots interpretation worked out 2:1 (Cu^{2+}/F^-) and 1:1 (CN^-) stoichiometry with sensor molecule. Sensor displayed strong binding affinity for Cu^{2+}/F^- compared to CN^- , as deduced from the B–H plots.

Additionally, deionized water or methanol, effectively discriminate the F^- ions with noticeable color variation from blue to orange/grey, respectively, in THF. Moreover, slight restoration of fluorescence was also observed. Contrary to this, with CN^- ions, complete quenching of emission intensity, with no visible naked eye color change, were encountered. Paper strip experimentation further established the practical applicability for on-site detection of ions in aqueous medium. Analysis of ions in the commercial commodities further established the competitive selectivity of sensor. Thus, sensor emerged out as an economical alternative for the aqueous analysis of Cu^{2+} , F^- and CN^- ions.

Acknowledgements

The research work was supported by the Mahidol University for postdoctoral fellowship and financially supported by the Thailand Research Fund (RSA5980018 and DPG6080001), the Center of Excellence for Innovation in Chemistry (PERCH-CIC), Office of the Higher Education Commission, Ministry of Education (OHEC), and the Nanotechnology Center (NANOTEC), NSTDA, Ministry of Science and Technology, Thailand, through its program of Center of Excellence Network.

Appendix A. Supplementary data

Supplementary data associated with this article can be found, in the online version, at <https://doi.org/10.1016/j.jphotochem.2018.03.018>.

References

- [1] L. Wan, Q. Shu, J. Zhu, S. Jin, N. Li, X. Chen, S. Chen, A new multifunctional Schiff-based chemosensor for mask-free fluorimetric and colorimetric sensing of F^- and CN^- , *Talanta* 152 (2016) 39–44.
- [2] H.J. Lee, S.J. Park, H.J. Sin, Y.J. Na, C. Kim, A selective colorimetric chemosensor with an electron-withdrawing group for multi-analytes CN^- and F^- , *New J. Chem.* 39 (2015) 3900–3907.
- [3] J.H. Hu, J.B. Li, J. Qi, Y. Sun, Selective colorimetric and turn-on fluorimetric detection of cyanide using an acylhydrazone sensor in aqueous media, *New J. Chem.* 39 (2015) 4041–4046.
- [4] P.D. Beer, P.A. Gale, Anion recognition and sensing the state of the art and future perspectives, *Angew. Chem. Int. Ed.* 40 (2001) 486–516.
- [5] S.K. Kim, J. Yoon, A new fluorescent PET chemosensor for fluoride ions, *Chem. Commun.* 7 (2002) 770–771.
- [6] C.F. Wan, Y.J. Chang, C.Y. Chien, Y.W. Sie, C.H. Hu, A.T. Wu, A new multifunctional Schiff base as a fluorescence sensor for Fe^{2+} and F^- ions, and a colorimetric sensor for Fe^{3+} , *J. Lumin.* 178 (2016) 115–120.
- [7] V.K. Harikrishnan, S.M. Basheer, N. Joseph, A. Sreekanth, Colorimetric and fluorimetric response of salicylaldehyde dithiosemicarbazone towards fluoride, cyanide and copper ions: spectroscopic and TD-DFT studies, *Spectrochim. Acta Part A: Mol. Biomol. Spectrosc.* 182 (2017) 160–167.
- [8] Q. Song, A. Bamesberger, L. Yang, H. Houtwed, H. Cao, Excimer-monomer switch: a reaction-based approach for selective detection of fluoride, *Analyst* 139 (2014) 3588–3592.
- [9] S. Chanmungkalakul, V. Ervithayasuporn, S. Hanprasit, M. Masik, N. Prigyaia, S. Kiatkamjornwong, Silsesquioxane cages as fluoride sensors, *Chem. Commun.* 53 (2017) 12108–12111.
- [10] R. Kunthom, P. Piyanuch, N. Wanichacheva, V. Ervithayasuporn, Cage-like silsesquioxanes bearing rhodamines as fluorescence Hg^{2+} sensors, *J. Photochem. Photobiol., A* 356 (2018) 248–255.
- [11] C. Suksai, T. Tuntulani, Chromogenic anion sensors, *Chem. Soc. Rev.* 32 (2003) 192–202.
- [12] G.J. Park, G.R. You, Y.W. Choi, C. Kim, A naked-eye chemosensor for simultaneous detection of iron and copper ions and its copper complex for colorimetric/fluorescent sensing of cyanide, *Sens. Actuators B* 229 (2016) 257–271.
- [13] A.S. Gupta, A. Garg, K. Paul, V. Luxami, Differential sensing of fluoride and cyanide ions by using Dicyano substituted benzimidazole probe, *J. Lumin.* 173 (2016) 165–170.
- [14] A.R. Chowdhury, B.G. Roy, S. Jana, T. Weyhermuller, P. Banerjee, A simple cleft shaped hydrazine-functionalized colorimetric new Schiff base chemoreceptor for selective detection of F^- in organic solvent through PET signaling: development of a chemoreceptor based sensor kit for detection of fluoride, *Sens. Actuator B* 241 (2017) 706–715.
- [15] M. Boiocchi, L.D. Boca, D.E. Gomez, L. Fabbrizzi, M. Licchelli, E. Monzani, Nature of urea-fluoride interaction: incipient and definitive proton transfer, *J. Am. Chem. Soc.* 126 (2004) 16507–16514.
- [16] S.V. Bhosale, M.B. Kalyankar, S.J. Langford, A core-substituted naphthalene diimide fluoride sensor, *Org. Lett.* 11 (2009) 5418–5421.
- [17] M.S. Kumar, S.L.A. Kumar, A. Sreekanth, Highly selective fluorogenic anion chemosensors: naked-eye detection of F^- and AcO^- ions in natural water using a test strip, *Anal. Methods* 5 (2013) 6401–6410.
- [18] Y. Fu, C. Fan, G. Liu, S. Pu, A colorimetric and fluorescent sensor for Cu^{2+} and F^- based on a diarylethene with a 1,8-naphthalimide Schiff base unit, *Sens. Actuators B* 239 (2017) 295–303.
- [19] N. Kumari, S. Jha, S. Bhattacharya, Colorimetric probes based on anthraimidazoleiones for selective sensing of fluoride and cyanide ion via intramolecular charge transfer, *J. Org. Chem.* 76 (2011) 8215–8222.
- [20] B. Garg, T. Bisht, S.M.S. Chauhan, 2,2′-Diaminoazo-benzene, a potential scaffold for the synthesis of bis-ureas and thioureas: solution phase anion sensing and binding studies, *Sens. Actuators B* 168 (2012) 318–328.
- [21] A. Bamesberger, C. Schwartz, Q. Song, W. Han, Z. Wang, H. Cao, Rational design of a rapid fluorescent approach for detection of inorganic fluoride in MeCN-H₂O: a new fluorescence switch based on N-aryl-1,8-naphthalimide, *New J. Chem.* 38 (2014) 884–888.
- [22] S.M. Kim, M. Kang, I. Choi, J.J. Lee, C. Kim, A highly selective colorimetric chemosensor for cyanide and sulfide in aqueous solution: experimental and theoretical studies, *New J. Chem.* 40 (2016) 7768–7778.
- [23] P.A. Gale, T. Gunnlaugsson, Preface: supramolecular chemistry of anionic species themed issue, *Chem. Soc. Rev.* 39 (2010) 3595–3596.
- [24] P.A. Gale, Anion receptor chemistry: highlights from 2008 and 2009, *Chem. Soc. Rev.* 39 (2010) 3746–3771.
- [25] Q. Wang, Y. Xie, Y. Ding, X. Li, W. Zhu, Colorimetric fluoride sensors based on deprotonation of pyrrole-hemiquinone compounds, *Chem. Commun.* 46 (2010) 3669–3671.
- [26] T. Gunnlaugsson, M. Glynn, G.M. Tocci, P.E. Kruger, F.M. Pfeffer, Anion recognition and sensing using luminescent and colorimetric sensors, *Coord. Chem. Rev.* 250 (2006) 3094–3117.
- [27] D. Udhayakumari, S. Velmathi, M.S. Boobalan, Novel chemosensor for multiple target anions: the detection of F^- and CN^- ion via different approach, *J. Fluor. Chem.* 175 (2015) 180–184.
- [28] Y.W. Choi, J.J. Lee, G.R. You, S.Y. Lee, C. Kim, Chromogenic naked-eye detection of copper ion and fluoride, *RSC Adv.* 5 (2015) 86463–86472.
- [29] X. Yang, W. Zhang, Z. Yi, H. Xu, J. Wei, L. Hao, Highly sensitive and selective fluorescent sensor for copper(II) based on salicylaldehyde Schiff-base derivatives with aggregation induced emission and mechanoluminescence, *New J. Chem.* 41 (2017) 11079–11088.
- [30] J.T. Yeh, P. Venkatesan, S.P. Wu, A highly selective turn-on fluorescent sensor for fluoride and its application in imaging of living cells, *New J. Chem.* 38 (2014) 6198–6204.
- [31] Y. Ma, Y. Zhao, F. Zhang, T. Jiang, X. Wei, H. Shen, R. Wang, Z. Shi, Two new chemosensors for fluoride ion based on perylene tetra-(alkoxycarbonyl) derivatives, *Sens. Actuators B* 241 (2017) 735–743.
- [32] E.J. Cho, B.J. Ryu, Y.J. Lee, K.C. Nam, Visible colorimetric fluoride ion sensors, *Org. Lett.* 7 (2005) 2607–2609.
- [33] A. Ghosh, K. Mukherjee, S.K. Ghosh, B. Saha, Sources and toxicity of fluoride in the environment, *Res. Chem. Intermed.* 39 (2013) 2881–2915.
- [34] Y. Fu, C. Fan, G. Liu, S. Pu, A colorimetric and fluorescent sensor for Cu^{2+} and F^- based on a diarylethene with a 1,8-naphthalimide Schiff base unit, *Sens. Actuators B* 239 (2017) 295–303.
- [35] Q. Gao, L. Ji, Q. Wang, K. Yin, J. Li, L. Chen, Colorimetric sensor for highly sensitive and selective detection of copper ion, *Anal. Methods* 9 (2017) 5094–5100.
- [36] G.T. Spence, P.D. Beer, Expanding the scope of the anion templated synthesis of interlocked structure, *Acc. Chem. Res.* 46 (2013) 571–586.
- [37] E.S. Figueroa, M.E. Moragues, E. Climent, A. Agostini, R.M. Manez, F. Sancenon, Chromogenic and fluorogenic chemosensors and reagents for anions. A comprehensive review of the years 2010–2011, *Chem. Soc. Rev.* 42 (2013) 3489–3613.
- [38] M.H. Lee, B. Yoon, J.S. Kim, J.L. Sessler, Naphthalimide trifluoroacetyl acetate: a hydrazine-selective chemodosimetric sensor, *Chem. Sci.* 4 (2013) 4121–4126.
- [39] M. Kumar, N. Kumar, V. Bhalla, A naphthalimide based chemosensor for Zn^{2+} , pyrophosphate and H_2O_2 : sequential logic operations at the molecular level, *Chem. Commun.* 49 (2013) 877–879.
- [40] T.I. Kasher, A.H.E. Sehli, Synthesis characterization, antimicrobial and anticancer activity of Zn(II), Pd(II) and Ru(III) complexes of dehydroacetic acid hydrazine, *J. Chem. Pharm. Res.* 5 (2013) 474–483.
- [41] S. Kannan, M. Sivagamasundari, R. Ramesh, Y. Liu, Ruthenium(II) carbonyl complexes of dehydroacetic acid thiosemicarbazone: synthesis, structure, light emission and biological activity, *J. Organomet. Chem.* 693 (2008) 2251–2257.
- [42] Z. Zhang, J. Wu, Z. Shang, C. Wang, J. Cheng, X. Qian, Y. Xiao, Z. Xu, Y. Yang, Photocalibrated NO release from N-nitrosated naphthalimides upon one-photon or two-photon irradiation, *Anal. Chem.* 88 (2016) 7274–7280.
- [43] J. Gan, H. Tian, Z. Wang, K. Chen, J. Hill, P.A. Lane, M.D. Rahn, A.M. Fox, D.D.C. Bradley, Synthesis and luminescence properties of novel ferrocene-naphthalimides dyads, *J. Organomet. Chem.* 645 (2002) 168–175.
- [44] J.W. Pavlik, V. Ervithayasuporn, S. Tantayanon, Synthesis of some pyrano[2,3-c]pyrazoles, *J. Heterocycl. Chem.* 48 (2011) 710–714.
- [45] J.W. Pavlik, V. Ervithayasuporn, J.C. MacDonald, S. Tantayanon, The photochemistry of some pyranopyrazoles, *Arkivoc* 8 (2009) 57–68.

- [46] H. Yang, H. Song, Y. Zhu, S. Yang, Single chemosensor for multiple analytes: chromogenic and fluorogenic detection for fluoride anions and copper ions, *Tetrahedron Lett.* 53 (2012) 2026–2029.
- [47] K.D. Bhatt, H.S. Gupta, B.A. Makwana, D.J. Vyas, D. Maity, V.K. Jain, Calix receptor edifice; Scrupulous turn off fluorescent sensor for Fe(III), Co(II) and Cu (II), *J. Fluoresc.* 22 (2012) 1493–1500.
- [48] C.B. Murphy, Y. Zhang, T. Troxler, V. Ferry, J.J. Martin, W.E. Jones, Probing forster and dexter energy-transfer mechanisms in fluorescent conjugated polymer chemosensors, *J. Phys. Chem.* 108 (2004) 1537–1543.
- [49] A.S. Murugan, E.R.A. Noelson, J. Annaraj, Solvent dependent colorimetric, ratiometric dual sensor for copper and fluoride ions: real sample analysis, cytotoxicity and computational studies, *Inorg. Chem. Acta* 450 (2016) 131–139.
- [50] L. Zang, H. Shang, D. Wei, S. Jiang, A multi-stimuli-responsive organogel based on salicylidene Schiff base, *Sens. Actuators B* 185 (2013) 389–397.
- [51] W. Wang, Q. Wen, Y. Zhang, X. Fei, Y. Li, Q. Yang, X. Xu, Simple naphthalimide-based fluorescent sensor for highly sensitive and selective detection of Cd²⁺ and Cu²⁺ in aqueous solution and living cells, *Dalton Trans.* 42 (2013) 1827–1833.
- [52] Y.M. Hijji, B. Barare, A.P. Kennedy, R. Butcher, Synthesis and photophysical characterization of a Schiff base as anion sensor, *Sens. Actuators B* 136 (2009) 297–302.
- [53] V. Reena, S. Suganya, S. Velmathi, Synthesis and anion binding studies of azo-Schiff bases: selective colorimetric fluoride and acetate ion sensors, *J. Fluor. Chem.* 153 (2013) 89–95.
- [54] S. Mukherjee, A.K. Paul, Pyrene based chemosensor for selective sensing of fluoride in aprotic and protic environment, *J. Fluoresc.* 25 (2015) 1461–1467.
- [55] S.M. Kumar, K. Dhahagani, J. Rajesh, K. Anitha, G. Chakkaravarthi, N. Kanakachalam, M. Marappan, G. Rajagopal, Synthesis, structural analysis and cytotoxic effect of copper (II)-thiosemicarbazone complexes having heterocyclic bases: a selective naked eye sensor for F⁻ and CN⁻, *Polyhedron* 85 (2015) 830–840.
- [56] I.G. Shenderovich, H. Limbach, S.N. Smirnov, P.M. Tolstoy, G.S. Denisov, N.S. Golubev, H/D isotope effects on the low-temperature NMR parameters and hydrogen bond geometries of (FH)₂F⁻ and (FH)₃F⁻ dissolved in CDF₃/CDF₂Cl, *Phys. Chem. Chem. Phys.* 4 (2002) 5488–5497.